Smart Structures and Systems, *Vol. 26, No. 1* (*2020*) *77-87*
DOI: https://doi.org/10.12989/sss.2020.26.1.077

Static stability analysis of smart nonlocal thermo-piezo-magnetic plates via a quasi-3D formulation

Raad M. Fenjan [1], Ridha A. Ahmed [1], Nadhim M. Faleh*[1] and Fatima Masood Hani [2]

[1] *Al-Mustansiriah University*, *Engineering Collage P.O. Box 46049*, *Bab-Muadum*, *Baghdad 10001*, *Iraq*
[2] *Ministry of Construction and Housing*, *Iraq*

(*Received November 3, 2019, Revised April 6, 2020, Accepted April 28, 2020*)

Abstract. By employing a quasi-3D plate formulation, the present research studies static stability of magneto-electro-thermo-elastic functional grading (METE-FG) nano-sized plates. Accordingly, influences of shear deformations as well as thickness stretching have been incorporated. The gradation of piezo-magnetic and elastic properties of the nano-sized plate have been described based on power-law functions. The size-dependent formulation for the nano-sized plate is provided in the context of nonlocal elasticity theory. The governing equations are established with the usage of Hamilton's rule and then analytically solved for diverse magnetic-electric intensities. Obtained findings demonstrate that buckling behavior of considered nanoplate relies on the variation of material exponent, electro-magnetic field, nonlocal coefficient and boundary conditions.

Keywords: piezo-magnetic nanoplate; functional graded materials; thermal environments; buckling; quasi-3D plate theory; nonlocal theory

1. Introduction

An example for a smart material is piezoelectric-magnetic-elastic material in which magnetic-electric environments may lead to mechanical deformation (Aboudi 2001). This means that there is a coupling between magnetic-electric and elastic performances in such materials. In such materials, the material properties can be characterized by elastic, piezoelectric and magnetic constants. Structural components (beams, shells and plates) made of such smart materials are broadly utilized in actuators, sensors and intelligent systems. The material distribution in these structures may be homogenous or non-homogenous. When the material profile is variable thorough the thickness of a structure, the material distribution may be non-homogenous. As an example, a functional graded material is a non-homogenous material in which two materials are involved and all material properties change from one material to another (Li and Hu 2017a, b). Based on the percentage and volume fraction of each material, the complete behavior of the structure can be defined. There are several investigations on smart piezoelectric-magnetic-elastic structures having functionally graded distribution (Pan and Han 2005, Ramirez *et al*. 2006, Wu *et al*. 2010, Kattimani and Ray 2015).

According to recent experiments and atomistic simulations, it is reported that the mechanical character of nano-size piezo-electric and piezo-magnetic structures are relied on small scale effects. However, owning to the fact that classic continuum mechanical modelling is classified as a size free model, analyzing and investigating mechanical characteristics of small size structures based on the classic continuum theory yields inaccurate findings and accordingly wrongful designs. Howbeit, the atomistic modeling and molecular simulations are powerful tools for describing the size-dependent characteristics of small size structures, their application is not more economical because of the extra computational attempts. To prevail over such problems, a variety of size-dependent elasticity models including the nonlocal elasticity theory (Eringen and Edelen 1972, Eringen 1983), strains gradient elasticity theory (Alimirzaei *et al*. 2019) refined couple stresses theory and etc, are established for incorporating small size effects via standardizing some scale parameters and have been broadly exerted for the designing and study of the mechanical character of micro or nano structures (Zhu and Li 2017a, b, Ke and Wang 2014, Ke *et al*. 2014, Li *et al*. 2014, Farajpour *et al*. 2016). The smart material discussed in previous paragraph has been extensively applied in nano-structures and nano-devices. However, at the nanoscale, the behavior of structure is dissimilar to macro scale counterparts. This is owning to the existence of small size effects (Tounsi *et al*. 2013, Akbaş 2016, Barati 2017, Besseghier *et al*. 2017). Such small size effects are incorporated in non-classical elasticity theories such as Eringen's theory which is also used by other authors.

Finally, it can be mentioned that reported papers on buckling of magneto-electro-elastic plates are limited in the literature, especially those at nanoscale. In this article, critical buckling characteristics of MEE-FG nanoplates under magneto-electrical field are examined in the framework of a quasi-3D sinusoidal theory. The presented

*Corresponding author, Professor,
E-mail: dr.nadhim@uomustansiriyah.edu.iq;
drnadhim@gmail.com

ISSN: 1738-1584 (Print), 1738-1991 (Online)

model takes into account both shear deformations and thickness stretches impacts via high order variations of displacement components over the thickness. Material properties of nanoplate are graded in the lateral orientation according to the power-law modeling. The governing equations have been achieved via employment of Hamilton rule and Eringen's nonlocal elasticity and are solved via an analytical solution. The voluminous mathematical findings have been represented while the assertion is placed on studying the impacts of some factors such as external electrical voltages, magnetic potential, power-law indices and nonlocal factor on buckling properties of size-dependent MEE-FG nanoplates.

2. Theory of non-local elasticity for piezo-magnetic materials

According to the theory of non-local elasticity for smart magnetic-piezoelectric-elastic materials, stresses σ_{ij} electric displacement D_i and magnetic induction B_i can be defined in below form (Ansari and Gholami 2016)

$$\sigma_{ij} = \int_V \alpha(|x' - x|, \tau)\left[C_{ijkl}\varepsilon_{kl}(x') - e_{mij}E_m(x') - q_{nij}H_n(x') - C_{ijkl}\alpha_{kl}\Delta T\right]dV(x') \quad (1a)$$

$$D_i = \int_V \alpha(|x' - x|, \tau)\left[e_{ikl}\varepsilon_{kl}(x') + s_{im}E_m(x') + d_{in}H_n(x') - p_i\Delta T\right]dV(x') \quad (1b)$$

$$B_i = \int_V \alpha(|x' - x|, \tau)\left[q_{ikl}\varepsilon_{kl}(x') + d_{im}E_m(x') + \chi_{in}H_n(x') - \lambda_i\Delta T\right]dV(x') \quad (1c)$$

Above relations are associated with strains ε_{kl}, and electric-magnetic field (E_m, H_n). Till to now, mechanical analysis of piezo-magnetic nano-structures is performed based on diverse values for nonlocal parameter. Some of papers used actual value of nonlocal parameter with unit of nm, but some papers used normalized values for nonlocal factor in such a way that nonlocal parameter is normalized with respect to the length of nano-structure. Ke and Wang (2014) used normalized values for nonlocal parameter as $\mu = e_0a/L = 0.1\sim0.3$ for studying vibrations of smart nanobeams with length L. Also, Ansari and Gholami (2016) used normalized values for nonlocal parameter as $\mu = e_0a/a = 0.02\sim0.04$ to investigate nonlinear vibrations of smart nanoplates with length a.

All ingredients of stress field, electrical field displacement (D_i) and magnetic induction (B_i) for a size-dependent plate relevant to nonlocal theory may be written as

$$\sigma_{ij} - (e_0a)^2\nabla^2\sigma_{ij} = C_{ijkl}\varepsilon_{kl} - e_{mij}E_m - q_{nij}H_n - C_{ijkl}\alpha_{kl}\Delta T \quad (2a)$$

$$D_i - (e_0a)^2\nabla^2 D_i = e_{ikl}\varepsilon_{kl} + s_{im}E_m + d_{in}H_n - p_i\Delta T \quad (2b)$$

$$B_i - (e_0a)^2\nabla^2 B_i = q_{ikl}\varepsilon_{kl} + d_{im}E_m + \chi_{in}H_n - \lambda_i\Delta T \quad (2c)$$

where ∇^2 is the Laplacian operator.

3. Governing equations

3.1 Power-law functional grading material (P-FGM) plate

Each material property (P) for a smart nanoplate shown in Fig. 1 can defined as

$$P = P_2V_2 + P_1V_1 \quad (3)$$

P_2 and P_1 define the material factors at top and bottom surfaces, V_2 and V_1 define the volume fractions of top and bottom surfaces which have below definition (Draiche *et al*. 2016, El-Haina *et al*. 2017, Abdelaziz *et al*. 2017, Addou *et al*. 2019, Bellifa *et al*. 2017a, b, Bouadi *et al*. 2018, 2019, Bourada *et al*. 2018, Kaci *et al*. 2018)

$$V_2 = \left(\frac{z}{h} + \frac{1}{2}\right)^p, \qquad V_1 = 1 - V_2 \quad (4)$$

where $(p \geq 0)$ define the material index which evaluates the material dispersion over the lateral orientation (Zarga *et al*. 2019, Zaoui *et al*. 2019). Next, the effective material properties for MEE-FG plate takes the below definition

$$P(z) = (P_2 - P_1)\left(\frac{z}{h} + \frac{1}{2}\right)^p + P_1 \quad (5)$$

In this study, the top surface with $z = +h/2$, is selected to be $CoFe_2O_4$, and the bottom surface with $z = -h/2$ is selected to be $BaTio_3$ and the details are provided in Table 1.

3.2 Basic equations

In order to develop linear elastic formulation for free vibrations of the nano-scale plate, well-known refined plate theory has been used in the present paper. Thus, the displacements of nano-scale plate (u_1, u_2, u_3) may be written based on axial (u) and transverse (w_b, w_s) field variables as (Bousahla *et al*. 2014, Bourada *et al*. 2015, Bennoun *et al*. 2016, Hebali *et al*. 2014, Khiloun *et al*. 2019, Mahmoudi *et al*. 2019, Meksi *et al*. 2019, Mokhtar *et al*. 2018, Semmah *et al*. 2019, Tlidji *et al*. 2019, Yazid *et al*. 2018, Youcef *et al*. 2018)

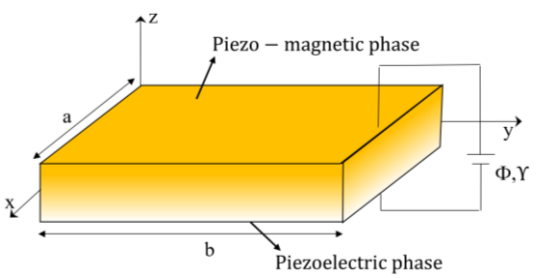

Fig. 1 A FG nano-size plate under magnetic-electrical field

Table 1 Magnetic-electric-elastic coefficients of the two phases (Ramirez *et al*. 2006)

Properties	$BaTiO_3$	$CoFe_2O_4$
$c_{11} = c_{22}$ (GPa)	166	286
c_{33}	162	269.5
$c_{13} = c_{23}$	78	170.5
c_{12}	77	173
c_{55}	43	45.3
c_{66}	44.5	56.5
e_{31} (Cm^{-2})	-4.4	0
e_{33}	18.6	0
e_{15}	11.6	0
q_{31} (N/Am)	0	580.3
q_{33}	0	699.7
q_{15}	0	550
s_{11} ($10^{-9}C^2m^{-2}N^{-1}$)	11.2	0.08
s_{33}	12.6	0.093
$\chi_{11}(10^{-6}Ns^2C^{-2}/2)$	5	-590
χ_{33}	10	157
$d_{11} = d_{22} = d_{33}$	0	0

$$u_1(x,y,z) = u(x,y) - z\frac{\partial w_b}{\partial x} - T(z)\frac{\partial w_s}{\partial x} \tag{6}$$

$$u_2(x,y,z) = v(x,y) - z\frac{\partial w_b}{\partial y} - T(z)\frac{\partial w_s}{\partial y} \tag{7}$$

$$u_3(x,y,z) = w_b(x,y) + w_s(x,y) + g(z)w_z(x,y) \tag{8}$$

in such a way that w_z defines transverse deflection related to thickness stretching. Based on a secant function, $T(z)$ defines shear function according to below definition

$$T(z) = z - z\,sec\left(\frac{rz}{h}\right) + z\,sec\left(\frac{r}{2}\right)\left[1 + \frac{r}{2}tan\left(\frac{r}{2}\right)\right], \quad r = 0.1 \tag{9}$$

Considering the fact that METE nano-scale plate is under electro-magnetic field with electrical potential (Φ) and magnetic potential (Υ), one can define the potentials in following forms as functions of electrical voltage (V_E) and magnetic potential intensity (Ω) (Ke and Wang 2014)

$$\Phi(x,y,z,t) = -cos(\xi z)\,\phi(x,y,t) + \frac{2z}{h}V \tag{10}$$

$$\Upsilon(x,y,z,t) = -cos(\xi z)\,\gamma(x,y,t) + \frac{2z}{h}\Omega \tag{11}$$

with $\xi = \pi/h$. Next, V and Ω define the exterior electrical voltages and magnetic potentials induced to the smart plate. For the refined plate formulation, the strain field including thickness stretching deflection (w_z) might be expressed by

$$\begin{Bmatrix}\varepsilon_x\\ \varepsilon_y\\ \varepsilon_z\\ \gamma_{xy}\end{Bmatrix} = \begin{Bmatrix}\varepsilon_x^0\\ \varepsilon_y^0\\ g'\varepsilon_z^0\\ \gamma_{xy}^0\end{Bmatrix} + z\begin{Bmatrix}\kappa_x^b\\ \kappa_y^b\\ 0\\ \kappa_{xy}^b\end{Bmatrix} + f\begin{Bmatrix}\kappa_x^s\\ \kappa_y^s\\ 0\\ \kappa_{xy}^s\end{Bmatrix}, \quad \begin{Bmatrix}\gamma_{yz}\\ \gamma_{xz}\end{Bmatrix} = g\begin{Bmatrix}\gamma_{yz}^s\\ \gamma_{xz}^s\end{Bmatrix}, \quad g = 1 - \frac{\partial f}{\partial z} \tag{12}$$

where

$$\begin{Bmatrix}\varepsilon_x^0\\ \varepsilon_y^0\\ \varepsilon_z^0\\ \gamma_{xy}^0\end{Bmatrix} = \begin{Bmatrix}\frac{\partial u}{\partial x}\\ \frac{\partial v}{\partial y}\\ w_z\\ \frac{\partial u}{\partial y} + \frac{\partial v}{\partial x}\end{Bmatrix}, \quad \begin{Bmatrix}\kappa_x^b\\ \kappa_y^b\\ \kappa_{xy}^b\end{Bmatrix} = \begin{Bmatrix}-\frac{\partial^2 w_b}{\partial x^2}\\ -\frac{\partial^2 w_b}{\partial y^2}\\ -2\frac{\partial^2 w_b}{\partial x \partial y}\end{Bmatrix}, \quad \begin{Bmatrix}\kappa_x^s\\ \kappa_y^s\\ \kappa_{xy}^s\end{Bmatrix} = \begin{Bmatrix}-\frac{\partial^2 w_s}{\partial x^2}\\ -\frac{\partial^2 w_s}{\partial y^2}\\ -2\frac{\partial^2 w_s}{\partial x \partial y}\end{Bmatrix}, \quad \begin{Bmatrix}\gamma_{yz}^s\\ \gamma_{xz}^s\end{Bmatrix} = \begin{Bmatrix}\frac{\partial w_s}{\partial y} + \frac{\partial w_z}{\partial y}\\ \frac{\partial w_s}{\partial x} + \frac{\partial w_z}{\partial x}\end{Bmatrix} \tag{13}$$

Calculating the three-dimensional gradient of electro-magnetic potentials gives the electrical field components (E_x, E_y, E_z) and magnet field components (H_x, H_y, H_z) as follows

$$E_x = -\Phi_{,x} = cos(\xi z)\frac{\partial \phi}{\partial x}, \tag{14}$$

$$E_y = -\Phi_{,y} = cos(\xi z)\frac{\partial \phi}{\partial y}, \tag{15}$$

$$E_z = -\Phi_{,z} = -\xi\,sin(\xi z)\,\phi - \frac{2V}{h} \tag{16}$$

$$H_x = -\Upsilon_{,x} = cos(\xi z)\frac{\partial \gamma}{\partial x}, \tag{17}$$

$$H_y = -\Upsilon_{,y} = cos(\xi z)\frac{\partial \gamma}{\partial y}, \tag{18}$$

$$H_z = -\Upsilon_{,z} = -\xi\,sin(\xi z)\,\gamma - \frac{2\Omega}{h} \tag{19}$$

Using Hamilton's rule, the equations of motion might be determined via

$$\int_0^t \delta(\Pi_S + \Pi_W)dt = 0 \tag{20}$$

Here Π_S defines strain energy, Π_W defines works done via exterior forces. The variation of strain energy might be written by

$$\delta\Pi_S = \int_v \sigma_{ij}\delta\varepsilon_{ij}dV = \int_v (\sigma_x\delta\varepsilon_x + \sigma_y\delta\varepsilon_y + \sigma_z\delta\varepsilon_z + \sigma_{xy}\delta\gamma_{xy} \tag{21a}$$

$$+\sigma_{yz}\delta\gamma_{yz}+\sigma_{xz}\delta\gamma_{xz}-D_x\delta E_x-D_y\delta E_y -D_z\delta E_z-B_x\delta H_x-B_y\delta H_y-B_z\delta H_z)dV \quad (21a)$$

Placing Eqs. (10) and (11) into Eq. (19) gives

$$\begin{aligned}\delta\Pi_S=\int_0^a\int_0^b\Big[&N_x\frac{\partial\delta u}{\partial x}-M_x^b\frac{\partial^2\delta w_b}{\partial x^2}-M_x^s\frac{\partial^2\delta w_s}{\partial x^2}\\&+N_y\frac{\partial\delta v}{\partial y}-M_y^b\frac{\partial^2\delta w_b}{\partial y^2}-M_y^s\frac{\partial^2\delta w_s}{\partial y^2}+R_z w_z\\&+N_{xy}\left(\frac{\partial\delta u}{\partial y}+\frac{\partial\delta v}{\partial x}\right)-2M_{xy}^b\frac{\partial^2\delta w_b}{\partial x\partial y}\\&-2M_{xy}^s\frac{\partial^2\delta w_s}{\partial x\partial y}+Q_{yz}\left(\frac{\partial\delta w_s}{\partial y}+\frac{\partial\delta w_z}{\partial y}\right)\\&+Q_{xz}\left(\frac{\partial\delta w_s}{\partial x}+\frac{\partial\delta w_z}{\partial x}\right)\Big]dxdy\\&+\int_0^a\int_0^b\int_{-\frac{h}{2}}^{\frac{h}{2}}\Big[-D_x\cos(\xi z)\delta\left(\frac{\partial\phi}{\partial x}\right)\\&-D_y\cos(\xi z)\delta\left(\frac{\partial\phi}{\partial y}\right)+D_z\xi\sin(\xi z)\delta\phi\\&-B_x\cos(\xi z)\delta\left(\frac{\partial\gamma}{\partial x}\right)-B_y\cos(\xi z)\delta\left(\frac{\partial\gamma}{\partial y}\right)\\&+B_z\xi\sin(\xi z)\delta\gamma\Big]dzdxdy\end{aligned} \quad (21b)$$

where

$$\left(N_i,M_i^b,M_i^s\right)=\int_A(1,z,T)\sigma_i\,dA,\quad i=(x,y,xy) \quad (22)$$

$$Q_i=\int_A g\sigma_i\,dA,\quad i=(xz,yz),\quad R_z=\int_A g'\sigma_z\,dA \quad (23)$$

The variation for works done by exterior forces might be determined as

$$\begin{aligned}\delta\Pi_W=\int_0^a\int_0^b\Big(&N_x^0\frac{\partial(w_b+w_s+g(z)w_z)}{\partial x}\frac{\partial\delta(w_b+w_s+g(z)w_z)}{\partial x}\\&+N_y^0\frac{\partial(w_b+w_s+g(z)w_z)}{\partial y}\frac{\partial\delta(w_b+w_s+g(z)w_z)}{\partial y}\\&+2\delta N_{xy}^0\frac{\partial(w_b+w_s+g(z)w_z)}{\partial x}\frac{\partial(w_b+w_s+g(z)w_z)}{\partial y}\Big)dxdy\end{aligned} \quad (24)$$

where N_x^0, N_y^0, N_{xy}^0 are membrane exerted forces. Herein, this is supposed that the METE-FG nano-sized plate is affected by outer electrical voltages and magnetic potentials; however, the shear forces have been discarded. Accordingly, $N_{xy}^0=0$ and N_x^0, N_y^0 define the in-plane loading owning to external electrical voltages V, magnetic potentials Ω, temperature field (T), respectively and are defined as

$$N_x^0=N_y^0=N^b+N^E+N^H+N^T \quad (25a)$$

$$\begin{aligned}N^E&=-\int_{-\frac{h}{2}}^{\frac{h}{2}}\tilde{e}_{31}\frac{2V}{h}dz,\qquad N^H=-\int_{-\frac{h}{2}}^{\frac{h}{2}}\tilde{q}_{31}\frac{2\Omega}{h}dz,\\N^T&=\int_{-h/2}^{h/2}c_{11}\alpha_1(T-T_0)dz,\end{aligned} \quad (25b)$$

For a METE nano-size plate, the governing equations based on refined plate theory and nonlocal stress effects may be expressed by

$$\frac{\partial N_x}{\partial x}+\frac{\partial N_{xy}}{\partial y}=0 \quad (26)$$

$$\frac{\partial N_{xy}}{\partial x}+\frac{\partial N_y}{\partial y}=0 \quad (27)$$

$$\begin{aligned}&\frac{\partial^2M_x^b}{\partial x^2}+2\frac{\partial^2M_{xy}^b}{\partial x\partial y}+\frac{\partial^2M_y^b}{\partial y^2}\\&-(N^b+N^E+N^H+N^T)\nabla^2(w_b+w_s+gw_z)=0\end{aligned} \quad (28)$$

$$\begin{aligned}&\frac{\partial^2M_x^s}{\partial x^2}+2\frac{\partial^2M_{xy}^s}{\partial x\partial y}+\frac{\partial^2M_y^s}{\partial y^2}+\frac{\partial Q_{xz}}{\partial x}+\frac{\partial Q_{yz}}{\partial y}\\&-(N^b+N^E+N^H)\nabla^2(w_b+w_s+gw_z)=0\end{aligned} \quad (29)$$

$$\begin{aligned}&\frac{\partial Q_{xz}}{\partial x}+\frac{\partial Q_{yz}}{\partial y}-R_z-g(N^b+N^E\\&+N^H+N^T)\nabla^2(w_b+w_s+gw_z)=0\end{aligned} \quad (30)$$

$$\int_{-\frac{h}{2}}^{\frac{h}{2}}\left(\cos(\xi z)\frac{\partial D_x}{\partial x}+\cos(\xi z)\frac{\partial D_y}{\partial y}+\xi\sin(\xi z)D_z\right)dz=0 \quad (31)$$

$$\int_{-\frac{h}{2}}^{\frac{h}{2}}\left(\cos(\xi z)\frac{\partial B_x}{\partial x}+\cos(\xi z)\frac{\partial B_y}{\partial y}+\xi\sin(\xi z)B_z\right)dz=0 \quad (32)$$

The constitutive equations can be expressed by

$$\begin{aligned}(1-\mu\nabla^2)\sigma_{xx}=&\tilde{C}_{11}\varepsilon_{xx}+\tilde{C}_{12}\varepsilon_{yy}+\tilde{C}_{13}\varepsilon_{zz}\\&-\tilde{e}_{31}E_z-\tilde{q}_{31}H_z-c_{11}\alpha_1\Delta T\end{aligned} \quad (33)$$

$$\begin{aligned}(1-\mu\nabla^2)\sigma_{yy}=&\tilde{C}_{12}\varepsilon_{xx}+\tilde{C}_{11}\varepsilon_{yy}+\tilde{C}_{13}\varepsilon_{zz}\\&-\tilde{e}_{31}E_z-\tilde{q}_{31}H_z\end{aligned} \quad (34)$$

$$\begin{aligned}(1-\mu\nabla^2)\sigma_{zz}=&\tilde{C}_{13}\varepsilon_{xx}+\tilde{C}_{13}\varepsilon_{yy}+\tilde{C}_{33}\varepsilon_{zz}\\&-\tilde{e}_{33}E_z-\tilde{q}_{33}H_z\end{aligned} \quad (35)$$

$$(1-\mu\nabla^2)\sigma_{xy}=\tilde{C}_{66}\gamma_{xy} \quad (36)$$

$$(1-\mu\nabla^2)\sigma_{xz}=\tilde{C}_{55}\gamma_{xz}-\tilde{e}_{15}E_x-\tilde{q}_{15}H_x \quad (37)$$

$$(1-\mu\nabla^2)\sigma_{yz}=\tilde{C}_{55}\gamma_{yz}-\tilde{e}_{15}E_y-\tilde{q}_{15}H_y \quad (38)$$

$$(1-\mu\nabla^2)D_x=\tilde{e}_{15}\gamma_{xz}+\tilde{s}_{11}E_x+\tilde{d}_{11}H_x \quad (39)$$

$$(1-\mu\nabla^2)D_y=\tilde{e}_{15}\gamma_{yz}+\tilde{s}_{11}E_y+\tilde{d}_{11}H_y \quad (40)$$

$$\begin{aligned}(1-\mu\nabla^2)D_z=&\tilde{e}_{31}\varepsilon_{xx}+\tilde{e}_{31}\varepsilon_{yy}+\tilde{e}_{33}\varepsilon_{zz}\\&+\tilde{s}_{33}E_z+\tilde{d}_{33}H_z\end{aligned} \quad (41)$$

$$(1-\mu\nabla^2)B_x = \tilde{q}_{15}\gamma_{xz} + \tilde{d}_{11}E_x + \tilde{\chi}_{11}H_x \tag{42}$$

$$(1-\mu\nabla^2)B_y = \tilde{q}_{15}\gamma_{yz} + \tilde{d}_{11}E_y + \tilde{\chi}_{11}H_y \tag{43}$$

$$\begin{aligned}(1-\mu\nabla^2)B_z = {}& \tilde{q}_{31}\varepsilon_{xx} + \tilde{q}_{31}\varepsilon_{yy} + \tilde{q}_{33}\varepsilon_{zz} \\ & + \tilde{d}_{33}E_z + \tilde{\chi}_{33}H_z\end{aligned} \tag{44}$$

So that μ is nonlocal scale factor; ΔT is temperature rise. Elastic, piezoelectric and magnetic material characteristics have been respectively marked by C_{ij}, e_{ij} and q_{ij}. For considering plane stress conditions, all material properties are expressed in a new form a follows

$$\begin{aligned}
&\tilde{C}_{11} = C_{11} - \frac{C_{13}^2}{C_{33}}, \quad \tilde{C}_{12} = C_{12} - \frac{C_{13}^2}{C_{33}}, \quad \tilde{C}_{66} = C_{66}, \\
&\tilde{e}_{15} = e_{15}, \qquad \tilde{e}_{31} = e_{31} - \frac{C_{13}e_{33}}{c_{33}}, \\
&\tilde{q}_{15} = q_{15}, \qquad \tilde{q}_{31} = q_{31} - \frac{C_{13}q_{33}}{C_{33}}, \\
&\tilde{d}_{11} = \tilde{d}_{11}, \qquad \tilde{d}_{33} = \tilde{d}_{33} + \frac{q_{33}e_{33}}{C_{33}}, \\
&\tilde{s}_{11} = s_{11}, \qquad \tilde{s}_{33} = s_{33} + \frac{e_{33}^2}{C_{33}}, \\
&\tilde{\chi}_{11} = \chi_{11}, \qquad \tilde{\chi}_{33} = \chi_{33} + \frac{q_{33}^2}{C_{33}}
\end{aligned} \tag{45}$$

By integration Eqs. (35)-(46) through the thickness direction, the below resultants for the nano-size plate would be derived:, as represented in Appendix. The governing equations of quasi-3D MEE-FG nanoplate based upon the displacement components and potential components might be achieved by placing Eqs. (A1)-(A9), into Eqs. (26)-(32) as

$$\begin{aligned}
&A_{11}\frac{\partial^2 u}{\partial x^2} + A_{66}\frac{\partial^2 u}{\partial y^2} + (A_{12}+A_{66})\frac{\partial^2 v}{\partial x\partial y} \\
&-B_{11}\frac{\partial^3 w_b}{\partial x^3} - (B_{12}+2B_{66})\frac{\partial^3 w_b}{\partial x\partial y^2} - B_{11}^s\frac{\partial^3 w_s}{\partial x^3} \\
&-(B_{12}^s+2B_{66}^s)\frac{\partial^3 w_s}{\partial x\partial y^2} + A_{31}^e\frac{\partial \phi}{\partial x} + A_{31}^m\frac{\partial \gamma}{\partial x} \\
&+X_{13}\frac{\partial w_z}{\partial x} = 0
\end{aligned} \tag{46}$$

$$\begin{aligned}
&A_{66}\frac{\partial^2 v}{\partial x^2} + A_{22}\frac{\partial^2 v}{\partial y^2} + (A_{12}+A_{66})\frac{\partial^2 u}{\partial x\partial y} \\
&-B_{22}\frac{\partial^3 w_b}{\partial y^3} - (B_{12}+2B_{66})\frac{\partial^3 w_b}{\partial x^2\partial y} - B_{22}^s\frac{\partial^3 w_s}{\partial y^3} \\
&-(B_{12}^s+2B_{66}^s)\frac{\partial^3 w_s}{\partial x^2\partial y} + A_{31}^e\frac{\partial \phi}{\partial y} + A_{31}^m\frac{\partial \gamma}{\partial y} \\
&+X_{13}\frac{\partial w_z}{\partial y} = 0
\end{aligned} \tag{47}$$

$$\begin{aligned}
&B_{11}\frac{\partial^3 u}{\partial x^3} + (B_{12}+2B_{66})\frac{\partial^3 u}{\partial x\partial y^2} \\
&+(B_{12}+2B_{66})\frac{\partial^3 v}{\partial x^2\partial y} + B_{22}\frac{\partial^3 v}{\partial y^3} - D_{11}\frac{\partial^4 w_b}{\partial x^4} \\
&+E_{31}^e\left(\frac{\partial^2 \phi}{\partial x^2}+\frac{\partial^2 \phi}{\partial y^2}\right) - A_{15}^e\left(\frac{\partial^2 \phi}{\partial x^2}+\frac{\partial^2 \phi}{\partial y^2}\right) \\
&-2(D_{12}+2D_{66})\frac{\partial^4 w_b}{\partial x^2\partial y^2} - D_{22}\frac{\partial^4 w_b}{\partial y^4} - D_{11}^s\frac{\partial^4 w_s}{\partial x^4} \\
&-2(D_{12}^s+2D_{66}^s)\frac{\partial^4 w_s}{\partial x^2\partial y^2} + E_{31}^m\left(\frac{\partial^2 \gamma}{\partial x^2}+\frac{\partial^2 \gamma}{\partial y^2}\right) \\
&-A_{15}^e\left(\frac{\partial^2 \gamma}{\partial x^2}+\frac{\partial^2 \gamma}{\partial y^2}\right) - D_{22}^s\frac{\partial^4 w_s}{\partial y^4} + Y_{13}\left(\frac{\partial^2 w_z}{\partial x^2}+\frac{\partial^2 w_z}{\partial y^2}\right) \\
&+(1-\mu\nabla^2)(-(N^b+N^E+N^H+N^T) \\
&\nabla^2(w_b+w_s+gw_z)) = 0
\end{aligned} \tag{48}$$

$$\begin{aligned}
&B_{11}^s\frac{\partial^3 u}{\partial x^3} + (B_{12}^s+2B_{66}^s)\frac{\partial^3 u}{\partial x\partial y^2} \\
&+(B_{12}^s+2B_{66}^s)\frac{\partial^3 v}{\partial x^2\partial y} + B_{22}^s\frac{\partial^3 v}{\partial y^3} - D_{11}^s\frac{\partial^4 w_b}{\partial x^4} \\
&-A_{15}^e\left(\frac{\partial^2 \phi}{\partial x^2}+\frac{\partial^2 \phi}{\partial y^2}\right) + A_{55}^s\frac{\partial^2 w_s}{\partial x^2} + A_{44}^s\frac{\partial^2 w_s}{\partial y^2} \\
&-2(D_{12}^s+2D_{66}^s)\frac{\partial^4 w_b}{\partial x^2\partial y^2} - D_{22}^s\frac{\partial^4 w_b}{\partial y^4} - H_{11}^s\frac{\partial^4 w_s}{\partial x^4} \\
&-2(H_{12}^s+2H_{66}^s)\frac{\partial^4 w_s}{\partial x^2\partial y^2} - H_{22}^s\frac{\partial^4 w_s}{\partial y^4} \\
&+F_{31}^e\left(\frac{\partial^2 \phi}{\partial x^2}+\frac{\partial^2 \phi}{\partial y^2}\right) + F_{31}^m\left(\frac{\partial^2 \gamma}{\partial x^2}+\frac{\partial^2 \gamma}{\partial y^2}\right) \\
&-A_{15}^m\left(\frac{\partial^2 \gamma}{\partial x^2}+\frac{\partial^2 \gamma}{\partial y^2}\right) + (A_{55}^s+Y_{13}^s)\frac{\partial^2 w_z}{\partial x^2} \\
&+(A_{44}^s+Y_{23}^s)\frac{\partial^2 w_z}{\partial y^2} + (1-\mu\nabla^2)(-(N^b+N^E \\
&+N^H+N^T)\nabla^2(w_b+w_s+gw_z)) = 0
\end{aligned} \tag{49}$$

$$\begin{aligned}
&-X_{13}\left(\frac{\partial u}{\partial x}+\frac{\partial v}{\partial y}\right) + Y_{13}\left(\frac{\partial^2 w_b}{\partial x^2}+\frac{\partial^2 w_b}{\partial y^2}\right) \\
&+Y_{13}^s\left(\frac{\partial^2 w_s}{\partial x^2}+\frac{\partial^2 w_s}{\partial y^2}\right) + A_{44}^s\left(\frac{\partial^2 w_s}{\partial y^2}+\frac{\partial^2 w_z}{\partial y^2}\right) \\
&+A_{55}^s\left(\frac{\partial^2 w_s}{\partial x^2}+\frac{\partial^2 w_z}{\partial x^2}\right) - Z_{33}w_z - H_{33}^e\phi - H_{33}^m\gamma \\
&+g(1-\mu\nabla^2)(-(N^b+N^E+N^H) \\
&\nabla^2(w_b+w_s+gw_z)) = 0
\end{aligned} \tag{50}$$

$$\begin{aligned}
&A_{31}^e\left(\frac{\partial u}{\partial x}+\frac{\partial v}{\partial y}\right) - E_{31}^e\left(\frac{\partial^2 w_b}{\partial x^2}+\frac{\partial^2 w_b}{\partial y^2}\right) \\
&-(F_{31}^e-E_{15}^e)\left(\frac{\partial^2 w_s}{\partial x^2}+\frac{\partial^2 w_s}{\partial y^2}\right) + F_{11}^e(\frac{\partial^2 \phi}{\partial x^2}+\frac{\partial^2 \phi}{\partial y^2}) \\
&+F_{11}^m\left(\frac{\partial^2 \gamma}{\partial x^2}+\frac{\partial^2 \gamma}{\partial y^2}\right) + H_{33}^e w_z - F_{33}^e\phi - F_{33}^m\gamma = 0
\end{aligned} \tag{51}$$

$$\begin{aligned}
&A_{31}^m\left(\frac{\partial u}{\partial x}+\frac{\partial v}{\partial y}\right) - E_{31}^m\left(\frac{\partial^2 w_b}{\partial x^2}+\frac{\partial^2 w_b}{\partial y^2}\right) \\
&-(F_{31}^m-E_{15}^m)\left(\frac{\partial^2 w_s}{\partial x^2}+\frac{\partial^2 w_s}{\partial y^2}\right) + F_{11}^m\left(\frac{\partial^2 \phi}{\partial x^2}+\frac{\partial^2 \phi}{\partial y^2}\right) \\
&+X_{11}^m\left(\frac{\partial^2 \gamma}{\partial x^2}+\frac{\partial^2 \gamma}{\partial y^2}\right) + H_{33}^m w_z - F_{33}^m\phi - X_{33}^m\gamma = 0
\end{aligned} \tag{52}$$

4. Solution procedure

Based on Galerkin's method, it is possible to provide a solution for buckling problem of quasi-3D piezo-magnetic

nanoplates based on the boundary conditions:

- Simply-supported (S):

$$\begin{matrix} M_x = w_b = N_x = w_s = 0 & \text{when} & \text{x = 0, a} \\ M_y = w_b = N_y = w_s = 0 & \text{when} & \text{y = 0, b} \end{matrix} \quad (53)$$

In next step, the seven variables based on quasi-3D piezo-magnetic plate model can be defined by

$$u = \sum_{m=1}^{\infty}\sum_{n=1}^{\infty} U_{mn}\frac{\partial R_m(x)}{\partial x}R_n(y) \quad (54)$$

$$v = \sum_{m=1}^{\infty}\sum_{n=1}^{\infty} V_{mn}R_m(x)\frac{\partial R_n(y)}{\partial y} \quad (55)$$

$$w_b = \sum_{m=1}^{\infty}\sum_{n=1}^{\infty} W_{bmn}R_m(x)\,R_n(y) \quad (56)$$

$$w_s = \sum_{m=1}^{\infty}\sum_{n=1}^{\infty} W_{smn}R_m(x)\,R_n(y) \quad (57)$$

$$w_z = \sum_{m=1}^{\infty}\sum_{n=1}^{\infty} W_{zmn}R_m(x)\,R_n(y) \quad (58)$$

$$\phi = \sum_{m=1}^{\infty}\sum_{n=1}^{\infty} \Phi_{mn}R_m(x)\,R_n(y) \quad (59)$$

$$\gamma = \sum_{m=1}^{\infty}\sum_{n=1}^{\infty} \Upsilon_{mn}R_m(x)\,R_n(y) \quad (60)$$

where (U_{mn}, V_{mn}, W_{bmn}, W_{smn}, W_{zmn}, Φ_{mn}, γ_{mn}) define the max displacmemnts and the function $R(x) = sin(\alpha x)$ and $R(y) = sin(\beta y)$ are for simply-support boundary conditions ($\alpha = m\pi/a,\ \beta = n\pi/b$). By finding the coefficient of stiffness matrix from above equations, one can write

$$[K]_{7*7}\begin{bmatrix} U_{mn} \\ V_{mn} \\ W_{bmn} \\ W_{smn} \\ W_{zmn} \\ \Psi_{mn} \\ \Upsilon_{mn} \end{bmatrix} = 0 \quad (61)$$

The non-trivial solution has been achieved while the determinant of stiffness matrix is set to zero ($|K| = 0$) to find critical buckling loads. The non-dimension form of buckling load might be introduced by

$$\bar{N} = N^b\frac{a^2}{D_c}, \qquad D_c = c_{11}^u h^3 \quad (62)$$

5. Numerical findings and discussions

In this chapter, impacts of different factors such as magneto-electrical field, nonlocality, boundary conditions and material compositions on critical buckling loads of graded MEE nanoplates are examined. The length of nano-sized plate has been chosen to be a = 10 nm. For the confirmation purpose, critical buckling loads are compared with those of FG nanoplates presented by Sobhy (2015) and a worthy agreement is found according to the findings represented in Table 2. For the verification study, the material constants have been assumed as: E_c = 380 GPa, E_m = 70 GPa and $v_c = v_m = 0.3$.

Table 2 Comparing the critical buckling loads of simple-supported graded nano-size plates (b = a, a = 10 h)

	μ = 0 nm²		μ = 2 nm²	
Material exponent (p)	Sobhy (2015)	Present	Sobhy (2015)	Present
0	18.6876	18.6877	10.4425	10.4426
0.5	10.0638	10.0638	5.6235	5.62359
2.5	6.2593	6.25935	3.4976	3.49769
10.5	4.9677	4.96776	2.7759	2.77596

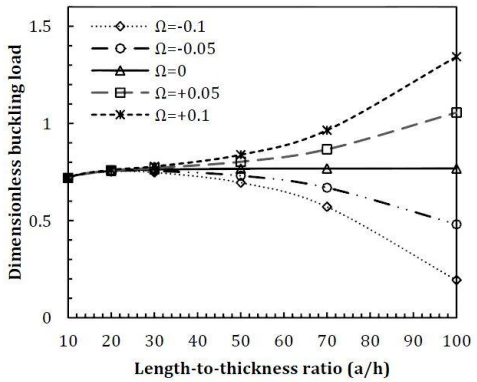

Fig. 2 Buckling load curves of the nano-size plate against length-to-thickness ratios based upon diverse magnetic intensities (p = 1, μ = 1 nm², V = 0×10⁻⁴)

Depicted in Fig. 2 is the buckling load of the graded piezo-magnetic nanoplate with the changes of length to thickness ratios (a/h) based on various magnetic potentials. There is no change in buckling load versus a/h when the magnetic potential is zero. Also, applying positive of negative magnetic potentials may increase or reduce the buckling load with respect to a/h.

In Figs. 3 and 4, changing of non-dimension buckling loads of graded MEE nanoplates vesus power-law index (p) is illustrated for different electrical voltages and magnetic potentials when a = 100 h and μ = 0.5 nm². This is deduced that critical buckling forces of graded MEE nano-size plate are significantly influenced by the magnitude and sign of magnetic and electric potentials for each values of power-law index. It is concluded that negative magnitudes for magnetic potentials give lower buckling forces than positive magnetic intensity factor. While, smaller magnitudes of electrical voltages result in greater buckling forces. Actually, the imposed negative/positive magnetic intensities might generate the in-plane compressive and tensile forces. Whereas, electrical fields show an opposite influence. It is also found that larger magnitudes of power-law index have

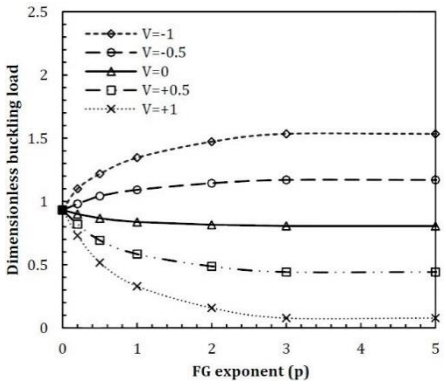

Fig. 3 Buckling load curves of the nano-size plate against gradient index for diverse electrical voltages (a = 100 h, ΔT = 0, $\Omega = 0\times10^{-5}$, μ = 0.5 nm^2)

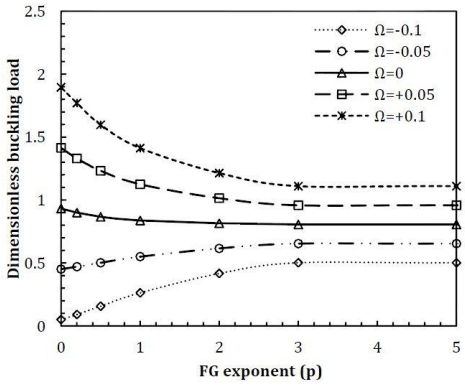

Fig. 4 Buckling load curves of the nano-size plate against gradient index for diverse magnetic intensity (a = 100 h, μ = 0.5 nm^2, ΔT = 0, $V = 0\times10^{-4}$)

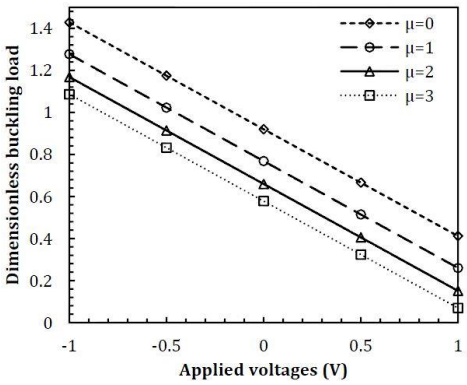

Fig. 5 Buckling load curves of the nano-size plate against applied voltages for diverse nonlocal factors (a = 100 h, ΔT = 20 K, p = 1, Ω = 0)

no sensible influence on buckling loads. But, smaller magnitudes of power-law index show more significant effect on the variations of buckling forces. Also, this is assumed that the value of electrical and magnetic intensities become equal to zero at the ends of the FG nanoplate.

Figs. 5 and 6 illustrate the variations of critical buckling loads of graded MEE nanoplate against electrical voltage and magnetic potential, respectively for different nonlocal

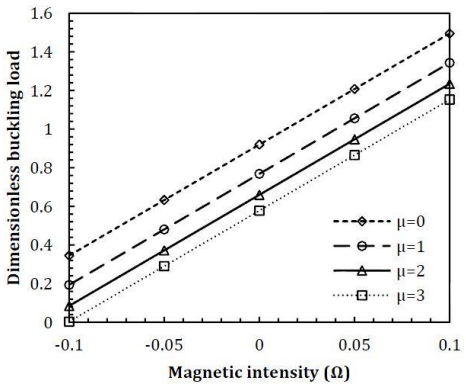

Fig. 6 Buckling load curves of the nano-size plate against magnetic intensity for diverse nonlocal factors (p = 1, a = 100 h, V = 0)

factors when p = 1 and a = 100 h. This is deduced that buckling forces of nonlocal graded MEE nano-size plate are often lower than that of local macro-size plate. Buckling loads decrease by the increment of the nonlocal factor at a constant magnetic intensity and electrical voltage. This incident is because of the reason that the low size impacts, that describe the reciprocal influences of every points within the area, might decline the strength of the nano-size structure. This is also deduced that as the electrical voltages and magnetic intensity change from negative to positive magnitudes, the critical buckling loads respectively reduce and increase.

6. Conclusions

Buckling characteristics of a quasi-3D piezo-magnetic nanoplate were reported in the present article. The complete formulation and solution for the problem based on quasi-3D plate model was presented. There was no change in buckling load versus side to thickness ratio when the magnetic potential was zero. Also, applying positive of negative magnetic potentials led to increasing or reducing the buckling load against length to thickness ratios. Also, this was reported that the buckling behaviors of the nano-sized plate is sensitive to material gradient exponent. Another observation was that size effects due to nonlocality changed significantly the buckling behaviors of piezo-magnetic nano-sized plate. Also, the dependency of buckling load to negative and positive voltages was clearly explained.

Acknowledgments

The authors would like to thank Mustansiriyah university (www.uomustansiriyah.edu.iq) Baghdad-Iraq for its support in the present work.

References

Abdelaziz, H.H., Meziane, M.A.A., Bousahla, A.A., Tounsi, A., Mahmoud, S.R. and Alwabli, A.S. (2017), "An efficient hyperbolic shear deformation theory for bending, buckling and

free vibration of FGM sandwich plates with various boundary conditions", *Steel Compos. Struct.*, *Int. J.*, **25**(6), 693-704. https://doi.org/10.12989/scs.2017.25.6.693

Aboudi, J. (2001), "Micromechanical analysis of fully coupled electro-magneto-thermo-elastic multiphase composites", *Smart Mater. Struct.*, **10**(5), 867. https://doi.org/10.1088/0964-1726/10/5/303

Addou, F.Y., Meradjah, M., Bousahla, A.A., Benachour, A., Bourada, F., Tounsi, A. and Mahmoud, S.R. (2019), "Influences of porosity on dynamic response of FG plates resting on Winkler/Pasternak/Kerr foundation using quasi 3D HSDT", *Comput. Concrete*, *Int. J.*, **24**(4), 347-367. https://doi.org/10.12989/cac.2019.24.4.347

Alimirzaei, S., Mohammadimehr, M. and Tounsi, A. (2019), "Nonlinear analysis of viscoelastic micro-composite beam with geometrical imperfection using FEM: MSGT electro-magneto-elastic bending, buckling and vibration solutions", *Struct. Eng. Mech.*, *Int. J.*, **71**(5), 485-502. https://doi.org/10.12989/sem.2019.71.5.485

Akbaş, Ş.D. (2016), "Forced vibration analysis of viscoelastic nanobeams embedded in an elastic medium", *Smart Struct. Syst.*, *Int. J.*, **18**(6), 1125-1143. https://doi.org/10.12989/sss.2016.18.6.1125

Ansari, R. and Gholami, R. (2016), "Size-dependent modeling of the free vibration characteristics of postbuckled third-order shear deformable rectangular nanoplates based on the surface stress elasticity theory", *Compos. Part B: Eng.*, **95**, 301-316. https://doi.org/10.1016/j.compositesb.2016.04.002

Barati, M.R. (2017), "Coupled effects of electrical polarization-strain gradient on vibration behavior of double-layered flexoelectric nanoplates", *Smart Struct. Syst.*, *Int. J.*, **20**(5), 573-581. https://doi.org/10.12989/sss.2017.20.5.573

Bellifa, H., Bakora, A., Tounsi, A., Bousahla, A.A. and Mahmoud, S.R. (2017a), "An efficient and simple four variable refined plate theory for buckling analysis of functionally graded plates", *Steel Compos. Struct.*, *Int. J.*, **25**(3), 257-270. https://doi.org/10.12989/scs.2017.25.3.257

Bellifa, H., Benrahou, K.H., Bousahla, A.A., Tounsi, A. and Mahmoud, S.R. (2017b), "A nonlocal zeroth-order shear deformation theory for nonlinear postbuckling of nanobeams", *Struct. Eng. Mech.*, *Int. J.*, **62**(6), 695-702. https://doi.org/10.12989/sem.2017.62.6.695

Bennoun, M., Houari, M.S.A. and Tounsi, A. (2016), "A novel five-variable refined plate theory for vibration analysis of functionally graded sandwich plates", *Mech. Adv. Mater. Struct.*, **23**(4), 423-431. https://doi.org/10.1080/15376494.2014.984088

Besseghier, A., Houari, M.S.A., Tounsi, A. and Mahmoud, S.R. (2017), "Free vibration analysis of embedded nanosize FG plates using a new nonlocal trigonometric shear deformation theory", *Smart Struct. Syst.*, *Int. J.*, **19**(6), 601-614. https://doi.org/10.12989/sss.2017.19.6.601

Bouadi, A., Bousahla, A.A., Houari, M.S.A., Heireche, H. and Tounsi, A. (2018), "A new nonlocal HSDT for analysis of stability of single layer graphene sheet", *Adv. Nano Res.*, *Int. J.*, **6**(2), 147-162. https://doi.org/10.12989/anr.2018.6.2.147

Boukhlif, Z., Bouremana, M., Bourada, F., Bousahla, A.A., Bourada, M., Tounsi, A. and Al-Osta, M.A. (2019), "A simple quasi-3D HSDT for the dynamics analysis of FG thick plate on elastic foundation", *Steel Compos. Struct.*, *Int. J.*, **31**(5), 503-516. https://doi.org/10.12989/scs.2019.31.5.503

Bourada, M., Kaci, A., Houari, M.S.A. and Tounsi, A. (2015), "A new simple shear and normal deformations theory for functionally graded beams", *Steel Compos. Struct.*, *Int. J.*, **18**(2), 409-423. https://doi.org/10.12989/scs.2015.18.2.409

Bourada, F., Amara, K., Bousahla, A.A., Tounsi, A. and Mahmoud, S.R. (2018), "A novel refined plate theory for stability analysis of hybrid and symmetric S-FGM plates", *Struct. Eng. Mech.*, *Int. J.*, **68**(6), 661-675. https://doi.org/10.12989/sem.2018.68.6.661

Bousahla, A.A., Houari, M.S.A., Tounsi, A. and Adda Bedia, E.A. (2014), "A novel higher order shear and normal deformation theory based on neutral surface position for bending analysis of advanced composite plates", *Int. J. Computat. Methods*, **11**(6), 1350082. https://doi.org/10.1142/S0219876213500825

Castrucci, P. (2014), "Carbon nanotube/silicon hybrid hetero-junctions for photovoltaic devices", *Adv. Nano Res.*, *Int. J.*, **2**(1), 23-56. https://doi.org/10.12989/anr.2014.2.1.023

Chemi, A., Heireche, H., Zidour, M., Rakrak, K. and Bousahla, A.A. (2015), "Critical buckling load of chiral double-walled carbon nanotube using non-local theory elasticity", *Adv. Nano Res.*, *Int. J.*, **3**(4), 193-206. https://doi.org/10.12989/anr.2015.3.4.193

Draiche, K., Tounsi, A. and Mahmoud, S.R. (2016), "A refined theory with stretching effect for the flexure analysis of laminated composite plates", *Geomech. Eng.*, *Int. J.*, **11**(5), 671-690. https://doi.org/10.12989/gae.2016.11.5.671

El-Haina, F., Bakora, A., Bousahla, A.A., Tounsi, A. and Mahmoud, S.R. (2017), "A simple analytical approach for thermal buckling of thick functionally graded sandwich plates", *Struct. Eng. Mech.*, *Int. J.*, **63**(5), 585-595. https://doi.org/10.12989/sem.2017.63.5.585

Eringen, A.C. (1983), "On differential equations of nonlocal elasticity and solutions of screw dislocation and surface waves", *J. Appl. Phys.*, **54**(9), 4703-4710. https://doi.org/10.1063/1.332803

Eringen, A.C. and Edelen, D.G.B. (1972), "On nonlocal elasticity", *J. Eng. Sci.*, **10**(3), 233-248. https://doi.org/10.1016/0020-7225(72)90039-0

Farajpour, A., Yazdi, M.H., Rastgoo, A., Loghmani, M. and Mohammadi, M. (2016), "Nonlocal nonlinear plate model for large amplitude vibration of magneto-electro-elastic nanoplates", *Compos. Struct.*, **140**, 323-336. https://doi.org/10.1016/j.compstruct.2015.12.039

Hebali, H., Tounsi, A., Houari, M.S.A., Bessaim, A. and Bedia, E.A.A. (2014), "New quasi-3D hyperbolic shear deformation theory for the static and free vibration analysis of functionally graded plates", *ASCE J. Eng. Mech.*, **140**, 374-383. https://doi.org/10.1061/(ASCE)EM.1943-7889.0000665

Jia, X.L., Zhang, S.M., Yang, J. and Kitipornchai, S. (2013), "Pull-in instability of electrically actuated poly-SiGe graded micro-beams", *Coupl. Syst. Mech.*, *Int. J.*, **2**(3), 215-230. https://doi.org/10.12989/csm.2013.2.3.215

Kaci, A., Houari, M.S.A., Bousahla, A.A., Tounsi, A. and Mahmoud, S.R. (2018), "Post-buckling analysis of shear-deformable composite beams using a novel simple two-unknown beam theory", *Struct. Eng. Mech.*, *Int. J.*, **65**(5), 621-631. https://doi.org/10.12989/sem.2018.65.5.621

Kattimani, S.C. and Ray, M.C. (2015), "Control of geometrically nonlinear vibrations of functionally graded magneto-electro-elastic plates", *Int. J. Mech. Sci.*, **99**, 154-167. https://doi.org/10.1016/j.ijmecsci.2015.05.012

Ke, L.L. and Wang, Y.S. (2014), "Free vibration of size-dependent magneto-electro-elastic nanobeams based on the nonlocal theory. *Physica E: Low-dimens. Syst. Nanostruct.*, **63**, 52-61. https://doi.org/10.1016/j.physe.2014.05.002

Ke, L.L., Wang, Y.S., Yang, J. and Kitipornchai, S. (2014), "Free vibration of size-dependent magneto-electro-elastic nanoplates based on the nonlocal theory", *Acta Mechanica Sinica*, **30**(4), 516-525. https://doi.org/10.1007/s10409-014-0072-3

Khiloun, M., Bousahla, A.A., Kaci, A., Bessaim, A., Tounsi, A. and Mahmoud, S.R. (2019), "Analytical modeling of bending and vibration of thick advanced composite plates using a four-variable quasi 3D HSDT", *Eng. Comput.* https://doi.org/10.1007/s00366-019-00732-1

Kumar, B.R. (2018), "Investigation on mechanical vibration of double-walled carbon nanotubes with inter-tube Van der waals

forces", *Adv. Nano Res., Int. J.*, **6**(2), 135-145. https://doi.org/10.12989/anr.2018.6.2.135

Li, L and Hu, Y. (2017a), "Torsional vibration of bi-directional functionally graded nanotubes based on nonlocal elasticity theory", *Compos. Struct.*, **172**, 242-250. https://doi.org/10.1016/j.compstruct.2017.03.097

Li, L. and Hu, Y. (2017b), "Post-buckling analysis of functionally graded nanobeams incorporating nonlocal stress and microstructure-dependent strain gradient effects", *Int. J. Mech. Sci.*, **120**, 159-170. https://doi.org/10.1016/j.ijmecsci.2016.11.025

Li, Y.S., Cai, Z.Y. and Shi, S.Y. (2014), "Buckling and free vibration of magnetoelectroelastic nanoplate based on nonlocal theory", *Compos. Struct.*, **111**, 522-529. https://doi.org/10.1016/j.compstruct.2014.01.033

Mahmoudi, A., Benyoucef, S., Tounsi, A., Benachour, A., Adda Bedia, E.A. and Mahmoud, S.R. (2019), "A refined quasi-3D shear deformation theory for thermo-mechanical behavior of functionally graded sandwich plates on elastic foundations", *J. Sandw. Struct. Mater.*, **21**(6), 1906-1926. https://doi.org/10.1177/1099636217727577

Marani, R. and Perri, A.G. (2017), "An approach to model the temperature effects on IV characteristics of CNTFETs", *Adv. Nano Res., Int. J.*, **5**(1), 61-67. https://doi.org/10.12989/anr.2017.5.1.061

Meksi, R., Benyoucef, S., Mahmoudi, A., Tounsi, A., Adda Bedia, E.A. and Mahmoud, S.R. (2019), "An analytical solution for bending, buckling and vibration responses of FGM sandwich plates", *J. Sandw. Struct. Mater.*, **21**(2), 727-757. https://doi.org/10.1177/1099636217698443

Mokhtar, Y., Heireche, H., Bousahla, A.A., Houari, M.S.A., Tounsi, A. and Mahmoud, S.R. (2018), "A novel shear deformation theory for buckling analysis of single layer graphene sheet based on nonlocal elasticity theory", *Smart Struct. Syst., Int. J.*, **21**(4), 397-405. https://doi.org/10.12989/sss.2018.21.4.397

Pan, E. and Han, F. (2005), "Exact solution for functionally graded and layered magneto-electro-elastic plates", *Int. J. Eng. Sci.*, **43**(3), 321-339. https://doi.org/10.1016/j.ijengsci.2004.09.006

Ramirez, F., Heyliger, P.R. and Pan, E. (2006), "Discrete layer solution to free vibrations of functionally graded magneto-electro-elastic plates", *Mech. Adv. Mater. Struct.*, **13**(3), 249-266. https://doi.org/10.1080/15376490600582750

Semmah, A., Heireche, H., Bousahla, A.A. and Tounsi, A. (2019), "Thermal buckling analysis of SWBNNT on Winkler foundation by non local FSDT", *Adv. Nano Res., Int. J.*, **7**(2), 89-98. https://doi.org/10.12989/anr.2019.7.2.089

Sobhy, M. (2015), "A comprehensive study on FGM nanoplates embedded in an elastic medium", *Composite Structures*, **134**, 966-980. https://doi.org/10.1016/j.compstruct.2015.08.102

Tlidji, Y., Zidour, M., Draiche, K., Safa, A., Bourada, M., Tounsi, A., Bousahla, A.A. and Mahmoud, S.R. (2019), "Vibration analysis of different material distributions of functionally graded microbeam", *Struct. Eng. Mech., Int. J.*, **69**(6), 637-649. https://doi.org/10.12989/sem.2019.69.6.637

Tounsi, A., Benguediab, S., Adda, B., Semmah, A. and Zidour, M. (2013), "Nonlocal effects on thermal buckling properties of double-walled carbon nanotubes", *Adv. Nano Res., Int. J.*, **1**(1), 1-11. https://doi.org/10.12989/anr.2013.1.1.001

Wu, C.P., Chen, S.J. and Chiu, K.H. (2010), "Three-dimensional static behavior of functionally graded magneto-electro-elastic plates using the modified Pagano method", *Mech. Res. Commun.*, **37**(1), 54-60. https://doi.org/10.1016/j.mechrescom.2009.10.003

Yazid, M., Heireche, H., Tounsi, A., Bousahla, A.A. and Houari, M.S.A. (2018), "A novel nonlocal refined plate theory for stability response of orthotropic single-layer graphene sheet resting on elastic medium", *Smart Struct. Syst., Int. J.*, **21**(1), 15-25. https://doi.org/10.12989/sss.2018.21.1.015

Youcef, D.O., Kaci, A., Benzair, A., Bousahla, A.A. and Tounsi, A. (2018), "Dynamic analysis of nanoscale beams including surface stress effects", *Smart Struct. Syst., Int. J.*, **21**(1), 65-74. https://doi.org/10.12989/sss.2018.21.1.065

Zaoui, F.Z., Ouinas, D. and Tounsi, A. (2019), "New 2D and quasi-3D shear deformation theories for free vibration of functionally graded plates on elastic foundations", *Compos. Part B*, **159**, 231-247. https://doi.org/10.1016/j.compositesb.2018.09.051

Zarga, D., Tounsi, A., Bousahla, A.A., Bourada, F. and Mahmoud, S.R. (2019), "Thermomechanical bending study for functionally graded sandwich plates using a simple quasi-3D shear deformation theory", *Steel Compos. Struct., Int. J.*, **32**(3), 389-410. https://doi.org/10.12989/scs.2019.32.3.389

Zenkour, A.M., Abouelregal, A.E., Alnefaie, K.A., Abu-Hamdeh, N.H. and Aifantis, E.C. (2014), "A refined nonlocal thermoelasticity theory for the vibration of nanobeams induced by ramp-type heating", *Appl. Mathe. Computat.*, **248**, 169-183. https://doi.org/10.1016/j.amc.2014.09.075

Zhang, Y.Q., Liu, G.R. and Xie, X.Y. (2005), "Free transverse vibrations of double-walled carbon nanotubes using a theory of nonlocal elasticity", *Phys. Rev. B*, **71**(19), 195404. https://doi.org/10.1103/PhysRevB.71.195404

Zhu, X. and Li, L. (2017a), "Longitudinal and torsional vibrations of size-dependent rods via nonlocal integral elasticity", *Int. J. Mech. Sci.*, **133**, 639-650. https://doi.org/10.1016/j.ijmecsci.2017.09.030

Zhu, X. and Li, L. (2017b), "Closed form solution for a nonlocal strain gradient rod in tension", *Int. J. Eng. Sci.*, **119**, 16-28. https://doi.org/10.1016/j.ijengsci.2017.06.019

CC

Appendix

$$
\begin{aligned}
&(1-\mu\nabla^2)\begin{Bmatrix}N_x\\N_y\\N_{xy}\end{Bmatrix}\\
&=\begin{pmatrix}A_{11}&A_{12}&0\\A_{12}&A_{22}&0\\0&0&A_{66}\end{pmatrix}\begin{Bmatrix}\dfrac{\partial u}{\partial x}\\\dfrac{\partial v}{\partial y}\\\dfrac{\partial u}{\partial y}+\dfrac{\partial v}{\partial x}\end{Bmatrix}\\
&+\begin{pmatrix}B_{11}&B_{12}&0\\B_{12}&B_{22}&0\\0&0&B_{66}\end{pmatrix}\begin{Bmatrix}-\dfrac{\partial^2 w_b}{\partial x^2}\\-\dfrac{\partial^2 w_b}{\partial y^2}\\-2\dfrac{\partial^2 w_b}{\partial x\partial y}\end{Bmatrix}\\
&+\begin{pmatrix}B_{11}^s&B_{12}^s&0\\B_{12}^s&B_{22}^s&0\\0&0&B_{66}^s\end{pmatrix}\begin{Bmatrix}-\dfrac{\partial^2 w_s}{\partial x^2}\\-\dfrac{\partial^2 w_s}{\partial y^2}\\-2\dfrac{\partial^2 w_s}{\partial x\partial y}\end{Bmatrix}\\
&+\begin{Bmatrix}X_{13}\\X_{23}\\0\end{Bmatrix}w_z+\begin{Bmatrix}A_{31}^e\\A_{31}^e\\0\end{Bmatrix}\phi+\begin{Bmatrix}A_{31}^m\\A_{31}^m\\0\end{Bmatrix}\gamma-\begin{Bmatrix}N_x^E\\N_y^E\\0\end{Bmatrix}\\
&-\begin{Bmatrix}N_x^H\\N_y^H\\0\end{Bmatrix}-\begin{Bmatrix}N^T\\N^T\\0\end{Bmatrix}
\end{aligned}
\tag{A1}
$$

$$
\begin{aligned}
&(1-\mu\nabla^2)\begin{Bmatrix}M_x^b\\M_y^b\\M_{xy}^b\end{Bmatrix}\\
&=\begin{pmatrix}B_{11}&B_{12}&0\\B_{12}&B_{22}&0\\0&0&B_{66}\end{pmatrix}\begin{Bmatrix}\dfrac{\partial u}{\partial x}\\\dfrac{\partial v}{\partial y}\\\dfrac{\partial u}{\partial y}+\dfrac{\partial v}{\partial x}\end{Bmatrix}\\
&+\begin{pmatrix}D_{11}&D_{12}&0\\D_{12}&D_{22}&0\\0&0&D_{66}\end{pmatrix}\begin{Bmatrix}-\dfrac{\partial^2 w_b}{\partial x^2}\\-\dfrac{\partial^2 w_b}{\partial y^2}\\-2\dfrac{\partial^2 w_b}{\partial x\partial y}\end{Bmatrix}\\
&+\begin{pmatrix}D_{11}^s&D_{12}^s&0\\D_{12}^s&D_{22}^s&0\\0&0&D_{66}^s\end{pmatrix}\begin{Bmatrix}-\dfrac{\partial^2 w_s}{\partial x^2}\\-\dfrac{\partial^2 w_s}{\partial y^2}\\-2\dfrac{\partial^2 w_s}{\partial x\partial y}\end{Bmatrix}\\
&+\begin{Bmatrix}Y_{13}\\Y_{23}\\0\end{Bmatrix}w_z+\begin{Bmatrix}E_{31}^e\\E_{31}^e\\0\end{Bmatrix}\phi+\begin{Bmatrix}E_{31}^m\\E_{31}^m\\0\end{Bmatrix}\gamma-\begin{Bmatrix}M_{bx}^E\\M_{by}^E\\0\end{Bmatrix}-\begin{Bmatrix}M_{bx}^H\\M_{by}^H\\0\end{Bmatrix}
\end{aligned}
\tag{A2}
$$

$$
\begin{aligned}
&(1-\mu\nabla^2)\begin{Bmatrix}M_x^s\\M_y^s\\M_{xy}^s\end{Bmatrix}\\
&=\begin{pmatrix}B_{11}^s&B_{12}^s&0\\B_{12}^s&B_{22}^s&0\\0&0&B_{66}^s\end{pmatrix}\begin{Bmatrix}\dfrac{\partial u}{\partial x}\\\dfrac{\partial v}{\partial y}\\\dfrac{\partial u}{\partial y}+\dfrac{\partial v}{\partial x}\end{Bmatrix}\\
&+\begin{pmatrix}D_{11}^s&D_{12}^s&0\\D_{12}^s&D_{22}^s&0\\0&0&D_{66}^s\end{pmatrix}\begin{Bmatrix}-\dfrac{\partial^2 w_b}{\partial x^2}\\-\dfrac{\partial^2 w_b}{\partial y^2}\\-2\dfrac{\partial^2 w_b}{\partial x\partial y}\end{Bmatrix}\\
&+\begin{pmatrix}H_{11}^s&H_{12}^s&0\\H_{12}^s&H_{22}^s&0\\0&0&H_{66}^s\end{pmatrix}\begin{Bmatrix}-\dfrac{\partial^2 w_s}{\partial x^2}\\-\dfrac{\partial^2 w_s}{\partial y^2}\\-2\dfrac{\partial^2 w_s}{\partial x\partial y}\end{Bmatrix}\\
&+\begin{Bmatrix}Y_{13}^s\\Y_{23}^s\\0\end{Bmatrix}w_z+\begin{Bmatrix}F_{31}^e\\F_{31}^e\\0\end{Bmatrix}\phi+\begin{Bmatrix}F_{31}^m\\F_{31}^m\\0\end{Bmatrix}\gamma-\begin{Bmatrix}M_{sx}^E\\M_{sy}^E\\0\end{Bmatrix}-\begin{Bmatrix}M_{sx}^H\\M_{sy}^H\\0\end{Bmatrix}
\end{aligned}
\tag{A3}
$$

$$
\begin{aligned}
(1-\mu\nabla^2)\begin{Bmatrix}Q_{xz}\\Q_{yz}\end{Bmatrix}&=\begin{pmatrix}A_{44}^s&0\\0&A_{55}^s\end{pmatrix}\begin{Bmatrix}\dfrac{\partial w_s}{\partial x}+\dfrac{\partial w_z}{\partial x}\\\dfrac{\partial w_s}{\partial y}+\dfrac{\partial w_z}{\partial y}\end{Bmatrix}\\
&-A_{15}^e\begin{Bmatrix}\dfrac{\partial\phi}{\partial x}\\\dfrac{\partial\phi}{\partial y}\end{Bmatrix}-A_{15}^m\begin{Bmatrix}\dfrac{\partial\gamma}{\partial x}\\\dfrac{\partial\gamma}{\partial y}\end{Bmatrix}
\end{aligned}
\tag{A4}
$$

$$
\begin{aligned}
&\int_{-\frac{h}{2}}^{\frac{h}{2}}(1-\mu\nabla^2)\begin{Bmatrix}D_x\\D_y\end{Bmatrix}cos(\xi z)dz\\
&=E_{15}^e\begin{Bmatrix}\dfrac{\partial w_s}{\partial x}\\\dfrac{\partial w_s}{\partial y}\end{Bmatrix}+F_{11}^e\begin{Bmatrix}\dfrac{\partial\phi}{\partial x}\\\dfrac{\partial\phi}{\partial y}\end{Bmatrix}+F_{11}^m\begin{Bmatrix}\dfrac{\partial\gamma}{\partial x}\\\dfrac{\partial\gamma}{\partial y}\end{Bmatrix}
\end{aligned}
\tag{A5}
$$

$$
\begin{aligned}
&(1-\mu\nabla^2)\int_{-\frac{h}{2}}^{\frac{h}{2}}D_z\xi\,sin(\xi z)dz\\
&=A_{31}^e\left(\frac{\partial u}{\partial x}+\frac{\partial v}{\partial y}\right)+H_{33}^e w_z-E_{31}^e\nabla^2 w_b\\
&-F_{31}^e\nabla^2 w_s-F_{33}^e\phi-F_{33}^m\gamma
\end{aligned}
\tag{A6}
$$

$$
\begin{aligned}
&\int_{-\frac{h}{2}}^{\frac{h}{2}}(1-\mu\nabla^2)\begin{Bmatrix}B_x\\B_y\end{Bmatrix}cos(\xi z)dz\\
&=E_{15}^m\begin{Bmatrix}\dfrac{\partial w_s}{\partial x}\\\dfrac{\partial w_s}{\partial y}\end{Bmatrix}+F_{11}^m\begin{Bmatrix}\dfrac{\partial\phi}{\partial x}\\\dfrac{\partial\phi}{\partial y}\end{Bmatrix}+X_{11}^m\begin{Bmatrix}\dfrac{\partial\gamma}{\partial x}\\\dfrac{\partial\gamma}{\partial y}\end{Bmatrix}
\end{aligned}
\tag{A7}
$$

$$\begin{aligned}&\int_{-\frac{h}{2}}^{\frac{h}{2}}(1-\mu\nabla^2)B_z\xi\,sin(\,\xi z)dz\\&=A_{31}^m\left(\frac{\partial u}{\partial x}+\frac{\partial v}{\partial y}\right)+H_{33}^m w_z-E_{31}^m\nabla^2 w_b\\&-F_{31}^m\nabla^2 w_s-F_{33}^m\phi-X_{33}^m\gamma\end{aligned}\tag{A8}$$

$$\begin{aligned}(1-\mu\nabla^2)R_z=X_{13}\left(\frac{\partial u}{\partial x}+\frac{\partial v}{\partial y}\right)+Z_{33}w_z-Y_{13}\nabla^2 w_b\\-Y_{13}^s\nabla^2 w_s+H_{33}^e\phi+H_{33}^m\gamma\end{aligned}\tag{A9}$$

so that it is possible to define the below relations

$$\begin{aligned}&\begin{Bmatrix}A_{11},B_{11},B_{11}^s,D_{11},D_{11}^s,H_{11}^s\\A_{12},B_{12},B_{12}^s,D_{12},D_{12}^s,H_{12}^s\\A_{66},B_{66},B_{66}^s,D_{66},D_{66}^s,H_{66}^s\end{Bmatrix}\\&=\int_{-h/2}^{h/2}\begin{Bmatrix}\tilde{C}_{11}\\\tilde{C}_{12}\\\tilde{C}_{66}\end{Bmatrix}(1,z,T,z^2,zT,T^2)\,dz\end{aligned}\tag{A10}$$

$$\{X_{13},Y_{13},Y_{13}^s\}=\int_{-h/2}^{h/2}\tilde{C}_{13}g'\{1,z,T\}\,dz\tag{A11}$$

$$\{Z_{33}\}=\int_{-h/2}^{h/2}\tilde{C}_{33}g'^2\,dz\tag{A12}$$

$$\{A_{31}^e,E_{31}^e,F_{31}^e\}=\int_{-h/2}^{h/2}\tilde{e}_{31}\xi\,sin(\,\xi z)\{1,z,T\}\,dz\tag{A13}$$

$$\{A_{31}^m,E_{31}^m,F_{31}^m\}=\int_{-h/2}^{h/2}\tilde{q}_{31}\xi\,sin(\,\xi z)\{1,z,T\}\,dz\tag{A14}$$

$$\{A_{15}^e,E_{15}^e\}=\int_{-h/2}^{h/2}\tilde{e}_{15}\,cos(\,\xi z)\{1,g\}\,dz\tag{A15}$$

$$\{A_{15}^m,E_{15}^m\}=\int_{-h/2}^{h/2}\tilde{q}_{15}\,cos(\,\xi z)\{1,g\}\,dz\tag{A16}$$

$$\{F_{11}^e,F_{33}^e\}=\int_{-h/2}^{h/2}\{\tilde{s}_{11}\,cos^2(\,\xi z),\tilde{s}_{33}\xi^2\,sin^2(\,\xi z)\}\,dz\tag{A17}$$

$$\{F_{11}^m,F_{33}^m\}=\int_{-h/2}^{h/2}\{\tilde{d}_{11}\,cos^2(\,\xi z),\tilde{d}_{33}\xi^2\,sin^2(\,\xi z)\}\,dz\tag{A18}$$

$$\{X_{11}^m,X_{33}^m\}=\int_{-h/2}^{h/2}\{\tilde{\chi}_{11}\,cos^2(\,\xi z),\tilde{\chi}_{33}\xi^2\,sin^2(\,\xi z)\}\,dz\tag{A19}$$

$$A_{44}^s=A_{55}^s=\int_{-h/2}^{h/2}\tilde{C}_{55}\,g^2dz\tag{A20}$$

Furthermore, in-plane force and moments associated with the magnetic-electric intensities in Eqs. (A1)-(A3) might be introduces as

$$\begin{aligned}N_x^E=N_y^E&=-\int_{-\frac{h}{2}}^{\frac{h}{2}}\tilde{e}_{31}\frac{2V}{h}dz\,,N_x^H=N_y^H\\&=-\int_{-h/2}^{h/2}\tilde{q}_{31}\frac{2\Omega}{h}dz\end{aligned}\tag{A21}$$

$$\begin{aligned}M_{bx}^E=M_{by}^E&=-\int_{-\frac{h}{2}}^{\frac{h}{2}}\tilde{e}_{31}\frac{2V}{h}zdz\,,M_{bx}^H=M_{by}^H\\&=-\int_{-h/2}^{h/2}\tilde{q}_{31}\frac{2\Omega}{h}zdz\end{aligned}\tag{A22}$$

$$\begin{aligned}M_{sx}^E=M_{sy}^E&=-\int_{-\frac{h}{2}}^{\frac{h}{2}}\tilde{e}_{31}\frac{2V}{h}f(z)dz\,,M_{sx}^H=M_{sy}^H\\&=-\int_{-h/2}^{h/2}\tilde{q}_{31}\frac{2\Omega}{h}f(z)dz\end{aligned}\tag{A23}$$